International Journal of Heat and Mass Transfer 91 (2015) 446–453

Contents lists available at ScienceDirect

International Journal of Heat and Mass Transfer

journal homepage: www.elsevier.com/locate/ijhmt

Flow boiling of refrigerant in horizontal metal-foam filled tubes: Part 1 – Two-phase flow pattern visualization

Yu Zhu [a,b], Haitao Hu [a], Shuo Sun [a], Guoliang Ding [a,*]

[a] Institute of Refrigeration and Cryogenics Engineering, Shanghai Jiao Tong University, Shanghai 200240, China
[b] Key Laboratory for Thermal Science and Power Engineering of Ministry of Education, Department of Thermal Engineering, Tsinghua University, Beijing 100084, China

ARTICLE INFO

Article history:
Received 23 July 2014
Received in revised form 24 June 2015
Accepted 23 July 2015
Available online 12 August 2015

Keywords:
Flow pattern
Metal foam
Two phase
Visualization

ABSTRACT

To better understanding the flow and heat transfer mechanisms of refrigerants flow boiling in metal-foam filled tubes, the two-phase flow patterns of R410A were observed in two 7.9 mm inner diameter horizontal tubes filled with 5 or 10 PPI (pores per inch) copper foams. The mass fluxes were 90–270 kg m^{-2} s^{-1}. The results show that slug flow, plug flow and annular flow occur in sequence with the increase of vapor quality. The transitions from slug to plug flow happen at lower vapor qualities with the increase of mass flux or metal foam PPI, while the transitions from plug to annular flow happen at vapor qualities around 0.4. The metal foam promotes the formation of annular flow and the effect is stronger with the higher PPI metal foam. A flow pattern map was developed that combines data from the present study and previous studies for flow patterns in metal-foam filled tubes.

1. Introduction

High porosity, open-cell metal foams have emerged as one of the most promising materials for heat transfer augmentation in recent years. They have been used to enhance boiling heat transfer rates [13,10,12,14,15], due to their excellent thermal features such as their large specific surface areas, high material thermal conductivities. The metal foams can be used to completely fill the tubes to enhance in-tube flow boiling heat transfer, because extending the metal foam to the tube center not only transfers the heat from the wall to the tube center, but also promotes turbulent flow. Recent research on flow boiling heat transfer in metal-foam filled tubes has shown that the heat transfer coefficients are increased 2–4 times compared with those in tubes without metal foams for the same working conditions [14,17]. Metal-foam filled tubes then may have potential applications in improving heat exchanger performance of refrigeration systems.

A prediction method for flow boiling heat transfer in metal-foam filled tubes should be proposed for using such kind of tubes in refrigeration systems. Among the prediction methods, some are flow pattern based heat transfer models which relate the flow patterns to the heat transfer coefficients, and show promise because the heat transfer mechanisms are clearly defined and the models are generally applicable to various conditions [3]. Therefore, studies of the two-phase flow patterns in metal-foam filled tubes are needed to understand the very complex flow boiling phenomena and to predict the heat transfer rates in such tubes.

Visualizations are commonly used to study two-phase flow patterns, and have been widely used in research on two-phase flow patterns in plain tubes without metal foam inside [7,11,4,5]. Flow field variations and phase interface movements can be observed by visualizations for two-phase flow pattern determination.

It is difficult to investigate two-phase flow patterns in metal-foam filled tubes by visualizations, because metal foam fibers may block the light. The existing research regarding two-phase flow patterns of refrigerants in metal-foam filled tubes used large diameter tubes (26 mm in [14], 23.4 mm in [17] and 13.8 mm in [16]) and there were many metal foam cells over a tube cross section, so the camera could not see what was in the metal foam structures. As a result, the two-phase flow patterns were all indirectly obtained by analyzing the wall temperature distributions. The wall temperature distributions can be used to describe the two-phase flow patterns, but the details of the flow behavior may be lost due to the absence of direct observations.

The two-phase flow patterns in metal-foam filled tubes can be visualized for smaller diameter tubes which are commonly used in typical refrigeration applications like air-conditioners, ventilators or fan-coil units, though it is not as easy as in smooth tubes. The smaller diameter tubes have fewer metal foam cells over a tube cross section, so the light can be transmitted through the voids in the metal foam. The present study investigates the

* Corresponding author.

http://dx.doi.org/10.1016/j.ijheatmasstransfer.2015.07.096
0017-9310/

two-phase flow patterns in metal-foam filled tubes using visualization.

2. Experimental facility for the flow pattern observation

2.1. Experimental rig

An experimental rig with the function of a refrigerant cycle and an efficient oil separation was built for observing the two-phase flow patterns of pure refrigerant in metal-foam filled tubes. The rig consists of a compressor, a condenser, an expansion valve, a preheater, test sections and a post heater as shown in Fig. 1. Three oil separators, an oil tank and a capillary tube were installed at the compressor outlet to separate the oil from the refrigerant vapor to ensure pure refrigerant flow through the test sections. In order to validate the effectiveness of the oil separators, three samples of the refrigerant-oil mixture at the condenser outlet were collected when the compressor was running at the highest frequency to get the maximum oil discharge rate from the compressor, and the oil concentrations of these samples were determined using a boiling-off-and-weight method based on ASHARE Standard 41.1. The average oil concentration of these samples is only 0.06%, meaning that the three oil separators worked well. The post heater superheated the refrigerant to ensure that the refrigerant entering the compressor was vapor.

A schematic diagram of the test section used for the visualization is also shown in Fig. 1. Two horizontal plexiglass tubes were fixed by two flanges at the tube ends. The outer plexiglass tube had a 30 mm inner diameter and a 3 mm wall thickness. The inner plexiglass tube had a 7.9 mm inner diameter which was the same as that of the copper tube connected to the plexiglass tube; and the wall thickness of the inner plexiglass tube was 5 mm which could bear pressures up to 1.5 MPa. The space between the two plexiglass tubes was evacuated to prevent water vapor in the air from condensing on the tube wall and obscuring the observations, and to prevent heat transfer between the refrigerant and the environment which would influence the flow pattern.

Two copper foams were used in the present study. Their sample pictures are shown in Fig. 2, and the structural parameters are list in Table 1. The PPI (pores per inch) and porosity are two independent structural parameters that the metal foam geometry, and can be used to calculate other metal foam structural parameters, such as the ligament diameter and specific surface area using Bhattacharya's model [2]. The length of copper-foam filled tube was 400 mm which is long enough to reduce the entrance effect according to [1].

The experimental equipment and instruments was described in detail in [6].

2.2. Working condition

The refrigerant was R410A which is widely used in refrigeration and air-conditioning systems. The saturation temperature was 7 °C. All the working conditions are tabulated in Table 2.

3. Results and discussion

3.1. Two-phase flow patterns observed in the metal-foam filled tubes

The two-phase flow patterns observed in the metal-foam filled tubes were classified according to the most commonly accepted terms and descriptions in smooth tubes, as in Zhao et al. [14]. The two-phase flow patterns in horizontal smooth tubes include stratified flow, stratified-wavy flow, plug flow, slug flow and annular flow. The flow behavior in the metal-foam filled tubes was somewhat different from that observed in smooth tubes for each

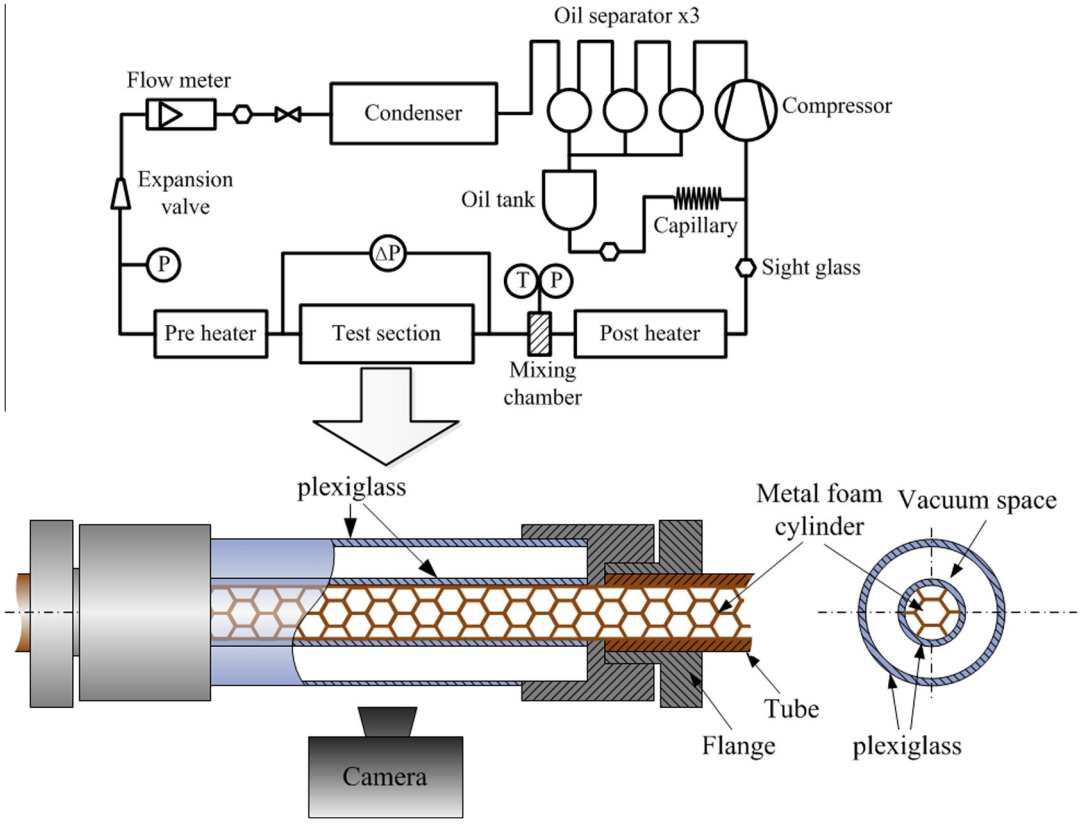

Fig. 1. Schematic diagram of the experimental rig and test section for visualization of two-phase flow patterns in metal-foam filled tubes.

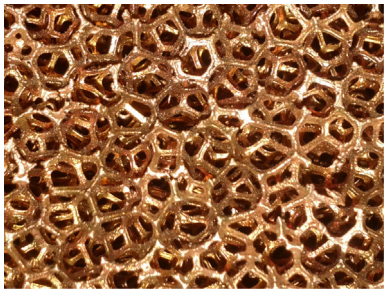

a) PPI = 5, porosity = 95%

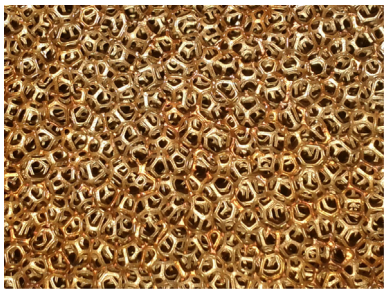

b) PPI = 10, porosity = 95%

Fig. 2. Photographs of the two copper foam samples.

flow pattern type due to the influence of the metal foam, but the topological structures of the phases in both tubes were similar for the same flow pattern due to the high porosity of the metal foams. Figs. 3–5 show the flow pattern images observed during the experiments, where the flow direction is from right to left (the arrows between the two images in Fig. 4 indicates how the flow patterns develop). Since the metal-foam filled tubes before the observation section were very long, the refrigerant flow in the observation section was fully developed.

3.1.1. Slug flow in the metal-foam tubes

Slug flow was observed at low vapor qualities and low mass fluxes in the metal-foam filled tubes.

Fig. 3 shows the slug flow in the metal-foam filled tubes where the liquid-phase refrigerant intermittently washes the top of the tube. The images show an interface between the liquid and the vapor. The interfaces are not smooth but are a little wavy due to the effect of the metal foam on the liquid flow. The metal foam also creates some droplets in the vapor, and some even touch the tube top surface. A comparison of Fig. 3a and b shows that the phase interface in the high PPI metal-foam tube is wavier than that in the low PPI one. Moreover, there is more liquid in the vapor in the high PPI metal-foam tube than in the low PPI one, because the higher PPI metal foam has more fibers and disrupts the flow field more.

The main difference between the slug flow in the metal-foam tubes and that in smooth tubes is the shape of the phase interface. In smooth tubes, the interface is formed by the surface tension and is smooth [9], while in the metal-foam tubes, the interface fluctuates because of metal foam fibers.

Table 1
Metal foam characteristic parameters.

Composition	Porosity (–)	PPI (–)	Ligament diameter (mm)	Specific surface area ($m^2\ m^{-3}$)
100 wt% Cu	95%	5	0.612	458
	95%	10	0.306	916

3.1.2. Plug flow in the metal-foam tubes

Plug flow was observed at low vapor qualities and moderate to high mass fluxes.

Fig. 4 shows the plug flow in the metal-foam tubes where the tube perimeter is wetted by liquid and the liquid refrigerant is well mixed with the bubbles that intermittently flow through the tube center. The left images of the two metal-foam filled tubes show that the liquid forms a continuous annular film around the tube perimeter as in annular flow. The right images show that the tube is sometimes fully filled with a liquid and vapor mixture. The left and right images appear in sequence in this flow pattern, which is similar to the plug flow in smooth tubes. The velocities for this flow pattern are much faster than for slug flow. The liquid at the tube bottom continuously touches the tube upper surface with the help of the metal foams. The vapor quality is not very high and the two-phase flow is intermittent.

The plug flow in the metal-foam tubes differs from and that in smooth tubes in that the phase interfaces of plug flow in smooth tubes are smooth, while those in the metal-foam tubes are vague due to the influence of the metal foam fibers. In addition, the liquid plugs that split the bubbles in smooth tubes have small bubbles dispersed in the liquid, while those in the metal-foam filled tubes are mixed more uniformly due to the influence of the metal foam fibers.

3.1.3. Annular flow in the metal-foam tubes

Annular flow was observed at high vapor qualities and all mass fluxes.

Fig. 5 shows the annular flow pattern in the metal-foam filled tubes with liquid films around the tube perimeter. This flow pattern was observed at high vapor qualities for all the mass fluxes. The images show that the liquid films at the tube bottom are thicker than those at the upper surface due to gravity.

The annular flow in the metal-foam tubes differs from that in smooth tubes as the liquid film surfaces fluctuate more in the metal-foam tubes because of the effect of metal foam fibers, and there is more liquid in the gas column at the center of the metal-foam tubes, as the liquid splashes into the vapor when encountering the metal foam fibers.

3.2. Transitions between two-phase flow patterns in metal-foam tubes

Fig. 6 shows the two-phase flow pattern distribution for the two metal-foam filled tubes used in this study. The two-phase flow patterns and their transitions have similar trends in both tubes. At low mass fluxes, the two-phase flow patterns exhibit slug flow at low vapor qualities and become annular flow at vapor qualities around 0.4. At moderate mass fluxes, the two-phase flow patterns are slug flow at very low vapor qualities, become plug flow at vapor qualities around 0.15–0.2 and then turn into annular flow at vapor qualities around 0.4. At high mass fluxes, the two-phase flow patterns are plug flow at low vapor qualities and become annular flow at vapor qualities around 0.4 as well.

Table 2
Working conditions.

Tube inner diameter (mm)	Saturation temperature (°C)	Mass flux ($kg\ m^{-2}\ s^{-1}$)	Heat flux ($kW\ m^{-2}$)	Vapor quality (–)
7.9	7	90	6.2	0.2–0.8
		135	9.3	
		180	12.4	
		225	15.5	
		270	18.6	

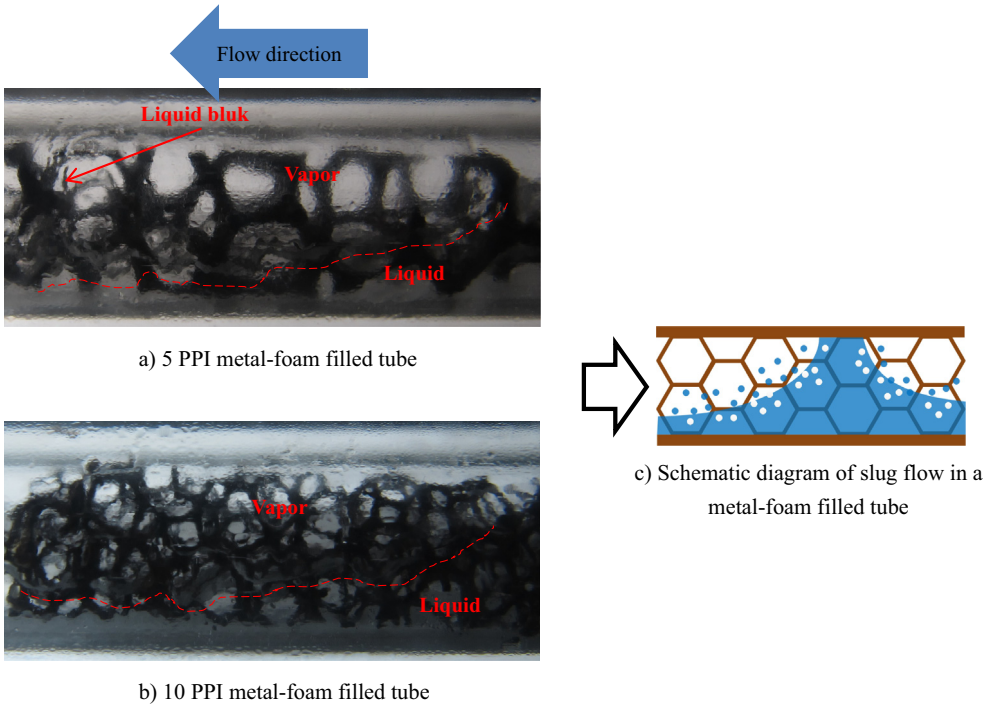

Fig. 3. Slug flow in metal-foam filled tubes.

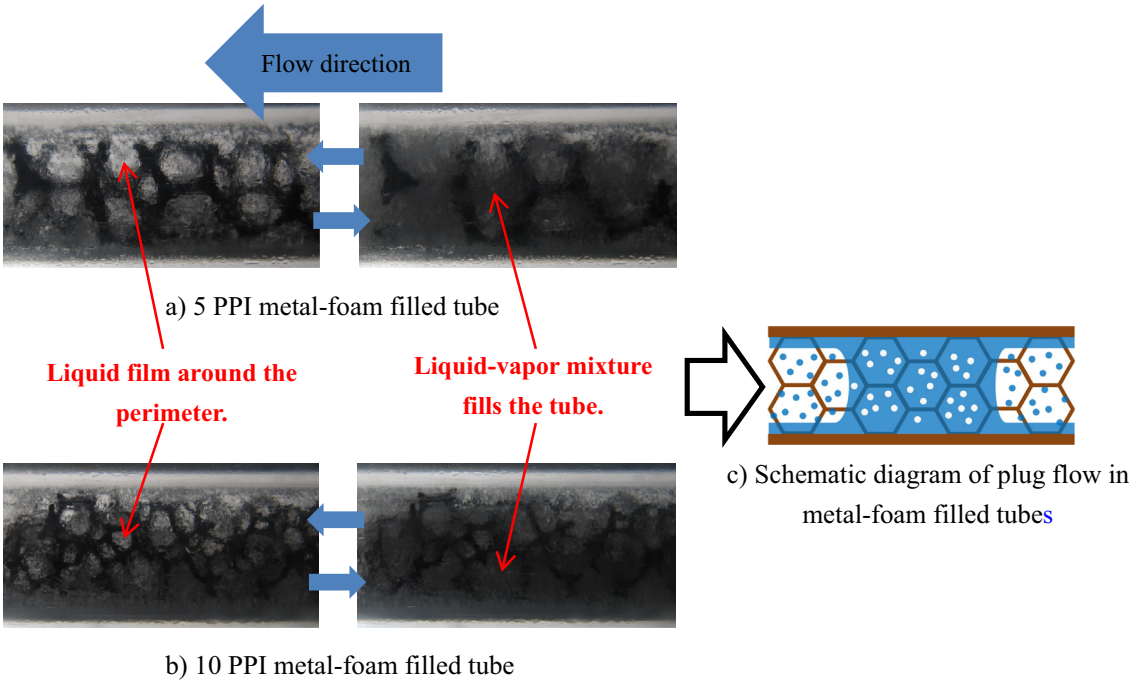

Fig. 4. Plug flow in metal-foam filled tubes.

3.3. Effect of the metal foam geometry on the flow pattern distributions

Fig. 7 shows the two-phase flow pattern transition criteria for the two metal-foam filled tubes. The transition criteria from plug flow to annular flow for the two metal-foam tubes are almost the same. Zhao et al. [14] had similar results with similar the transition criteria from slug/wavy flow to stratified-wavy flow for 20 PPI and 40 PPI metal-foam filled tubes. The ultrahigh porosity metal foams have little influence on the transition from intermittent flow (slug flow, plug flow, etc.) to non-intermittent flow (stratified flow, annular flow, etc.) and the transition is mainly influenced by the thermo-physical properties of the liquid and vapor.

The results in Fig. 7 also show that the transition between slug flow and plug flow for the 10 PPI metal-foam filled tube is earlier than for the 5 PPI foam. The structure of the higher PPI metal foam is more complex, so at low mass fluxes more liquid is conveyed to the upper part of the tube, thus plug flow occurs earlier.

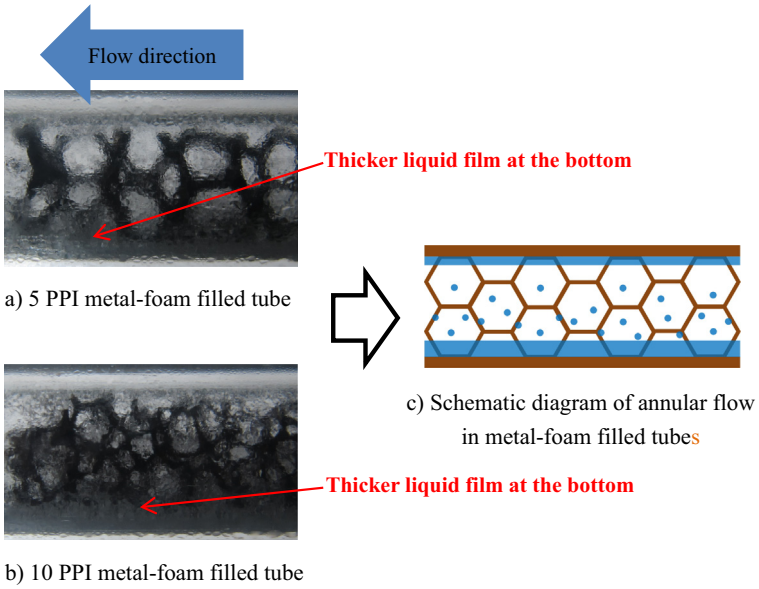

Fig. 5. Annular flow in metal-foam filled tubes.

3.4. Comparison of flow patterns in metal-foam filled and smooth tubes

Fig. 8 compares the two-phase flow pattern distributions for the two metal-foam filled tubes and a smooth tube with the same inner diameter. The flow patterns for the smooth tube were obtained using the method given by Wojtan et al. [11]. At low mass fluxes, the two-phase flow patterns exhibit slug flow at vapor qualities lower than 0.4 and stratified-wavy flow at vapor qualities higher than 0.4 in the smooth tube. The flow patterns in the metal-foam tubes also exhibit slug flow at low vapor qualities, because the flow velocities are low and the metal foam has little influence on the flow field. The increasing vapor quality increases both the vapor and liquid velocities so the metal foam has more influence on the flow. The metal foam fibers can even push liquid into the upper part of the tube to form annular flow.

At moderate mass fluxes, the two-phase flow patterns exhibit slug flow at vapor qualities lower than 0.4 and annular flow at vapor qualities higher than 0.4 in the smooth tube. The flow patterns in the metal-foam tubes also exhibit slug flow at low vapor qualities due to the low velocities of the refrigerant flow. The flow velocities are high enough with increasing vapor quality that the liquid is pushed to the tube perimeter forming annular flow. There are still some intermittent liquid plugs flowing through the tube at vapor qualities less than around 0.4, so plug flow occurs. At vapor qualities greater than 0.4, the two-phase flow pattern is annular flow which is similar to that in the smooth tube.

At high mass fluxes, the two-phase flow patterns in the smooth tube exhibit slug flow at vapor qualities lower than 0.4 and annular flow at higher qualities. The flow patterns in the metal-foam filled tubes are both plug flow, because the flow velocities at such mass fluxes are high enough so that the liquid is pushed to the tube wall. For vapor qualities larger than 0.4, the flow patterns in the metal-foam tubes are annular flow.

4. Two-phase flow pattern map of R410A in the metal-foam filled tubes

The two-phase flow pattern map and flow pattern transition criteria are of primary importance in understanding the flow boiling heat transfer mechanisms in tubes, so they should be identified to develop a flow-pattern based heat transfer model. There is only one two-phase flow pattern map for metal-foam filled tubes in the literature drawn based on the flow patterns obtained from wall temperature fluctuations of the tube [14]. The test used 26 mm inner diameter tubes filled with 20 or 40 PPI metal foams using R134a at mass fluxes of 26–106 kg m^{-2} s^{-1} and vapor qualities of 0–0.9. Their working conditions for their flow pattern map differ from those in this study. The existing research showed that the two-phase flow patterns are influenced by metal foam geometry. In this study, the tube diameter is smaller, the metal foam PPIs are smaller and the working fluid is R410A instead of R134a. The existing flow pattern map for metal-foam filled tubes may not be suitable for predicting the flow patterns for the present working conditions. The present two-phase flow pattern map drawn based on observations is compared with the existing flow pattern map.

4.1. Two-phase flow pattern map of R410A in metal-foam tubes

The flow patterns observed in the two metal-foam filled tubes in this study show that the metal foam geometry has little influence on the flow patterns. Moreover, the previous studies [16,17] investigated the two-phase flow patterns in tubes filled with metal foams with the same geometry of the present study at lower mass fluxes. The results showed that the flow was stratified flow at mass fluxes lower than 20 kg m^{-2} s^{-1} and slug/wavy flow or stratified-wavy flow at mass fluxes between 20 kg m^{-2} s^{-1} and 90 kg m^{-2} s^{-1}. Thus, the flow pattern distributions in Fig. 6a and b are combined with those in [16,17] for low mass fluxes in Fig. 9.

The flow patterns for different working conditions give rough transition criteria between the different flow patterns from Fig. 9, though the transition criteria may not be accurate due to the limited test conditions. The data in Fig. 9 shows that the transition from stratified flow to stratified-wavy flow occurs at mass fluxes around 20 kg m^{-2} s^{-1} and the transition from stratified-wavy flow to annular flow occurs at mass fluxes around 90 kg m^{-2} s^{-1}. In the flow pattern map for a smooth tube, the transition from intermittent to non-intermittent flow appears approximately at x_{IA} given by [7]. The line of x_{IA} separates the regions for intermittent flow

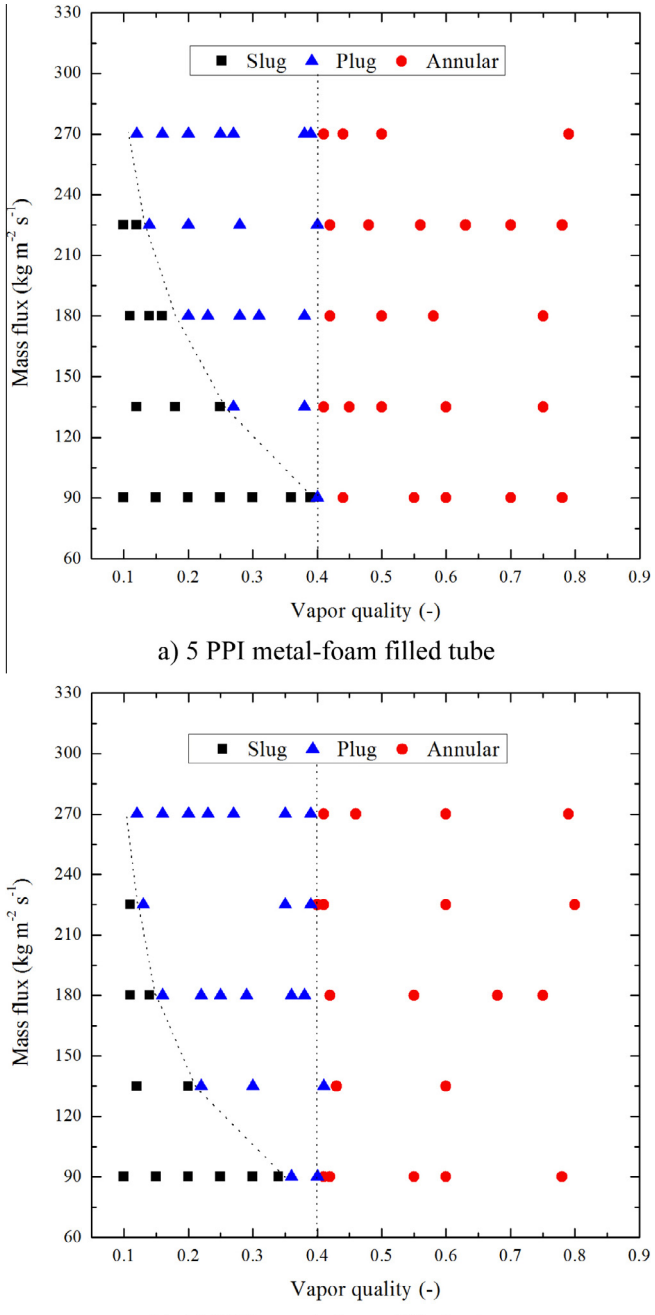

Fig. 6. Flow pattern distributions in metal-foam filled tubes.

from non-intermittent flow. This line is also used for the flow pattern map for the metal-foam filled tubes in this study and shows good agreement with the experimental results of the present work.

$$x_{IA} = \left\{ \left[0.291 \left(\frac{\rho_v}{\rho_l} \right)^{-0.571} \left(\frac{\mu_l}{\mu_v} \right)^{0.143} \right] + 1 \right\}^{-1} \quad (1)$$

where, ρ_v and ρ_l are the vapor and liquid refrigerant densities, respectively; μ_v and μ_l are the dynamic viscosities of the vapor and liquid refrigerant, respectively.

In summary, the two-phase flow pattern transition criteria for refrigerant flow boiling the metal-foam filled tubes at the conditions of this work are:

Stratified to stratified-wavy:	$G = 20$
Stratified-wavy to annular:	$G = 90$
Slug to slug/wavy:	$G = 142.9x + 31.42$
Slug to plug:	$G = 3052x^2 - 2147x + 458.4$
Plug to annular:	$x = 0.41$

where G is the mass flux, kg m^{-2} s^{-1}; x is the vapor quality.

4.2. Comparisons of the flow pattern map in this work with an existing map for metal-foam filled tubes

So far, there is one published literature reporting a flow pattern map for metal-foam filled tubes [8]. The working conditions in the existing study are different from those in this study, as shown in Table 3. The previous flow pattern map and the one drawn in this study are put together in Fig. 10 where the black dotted lines and the black font refer to the flow pattern map of this study, and the blue dotted lines and the blue font refer to the flow pattern map of the previous study. Some coherence and improvements between the two flow pattern maps for metal-foam filled tubes in the two studies can be found in Fig. 10.

The coherence includes: (1) Both flow pattern maps show plug/annular flow at mass fluxes above 100 kg m^{-2} s^{-1}, which means at mass fluxes above 100 kg m^{-2} s^{-1}, all the inner tube surface is always wetted by liquid. The phenomenon is attributed to the effect of the metal foam fibers on the liquid. (2) The transition criteria from intermittent flow (slug flow, plug flow, etc.) to non-intermittent flow (stratified flow, annular flow, etc.) is the same as in smooth tubes for both working fluids, which implies that the metal foam has little influence on the flow pattern transition from intermittent flow to non-intermittent flow, mainly due to the ultra-high porosities of the metal foams.

The improvements include: (1) The previous map did not have a stratified flow region, while the present map does. This is mainly because the lowest mass flux in the previous study was 26 kg m^{-2} s^{-1} and no stratified flow was observed at this mass flux; while the lowest mass flux in the present study was 10 kg m^{-2} s^{-1} and stratified flow was observed at this mass flux. (2) In the previous map, the flow was plug flow at low vapor qualities with high mass fluxes, while in the present map, the flow includes slug flow and plug flow in this region. The

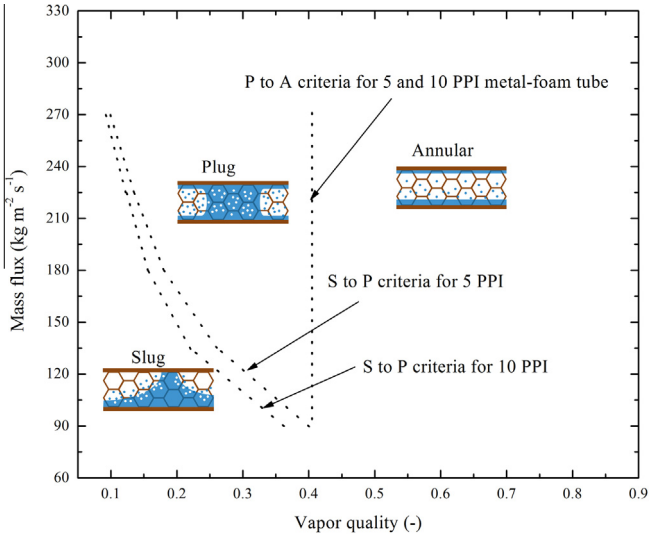

Fig. 7. Flow pattern maps for 5 PPI and 10 PPI metal-foam filled tubes.

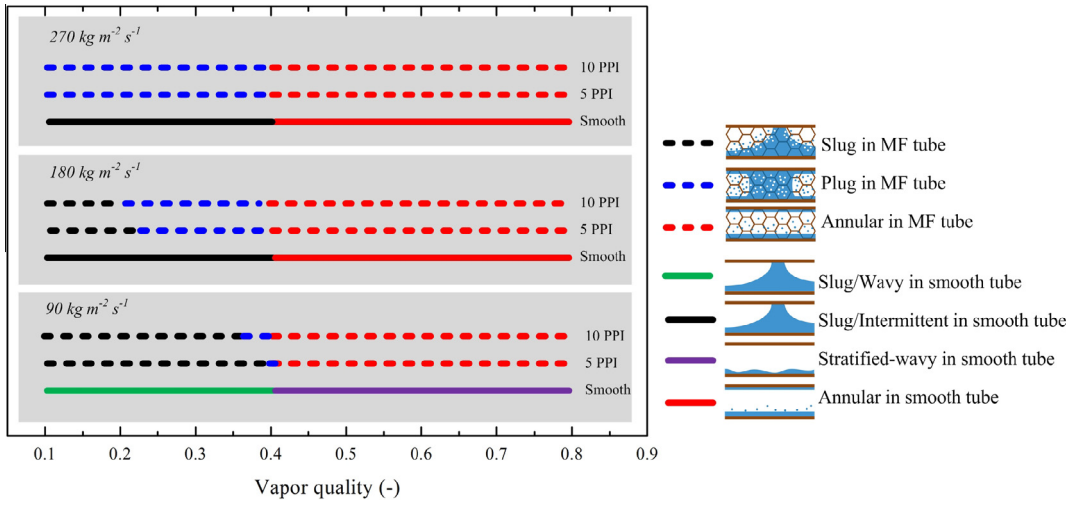

Fig. 8. Flow pattern maps for smooth and metal-foam filled tubes.

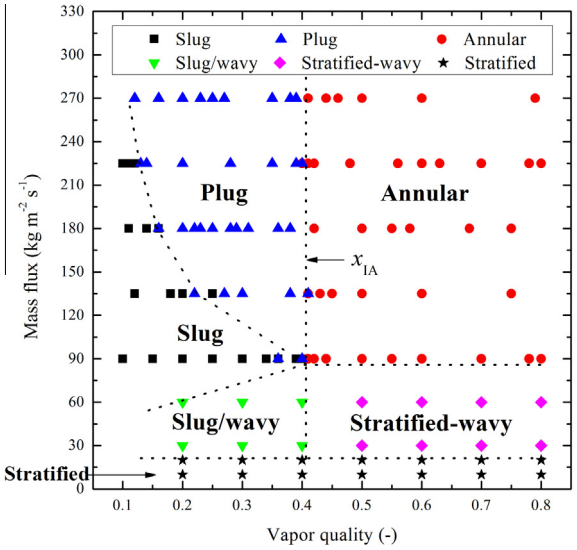

Fig. 9. Two-phase flow pattern map for metal-foam filled tubes.

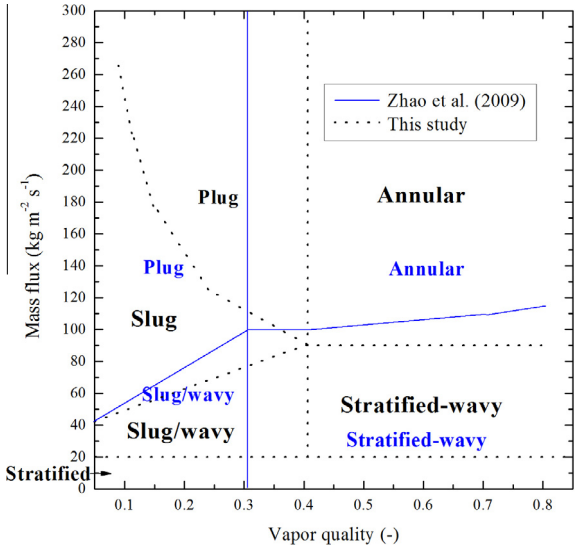

Fig. 10. Two-phase flow pattern map in this study and that in Lu and Zhao [8].

Table 3
Working conditions for a previous study and this study.

Working condition	This study	Lu and Zhao [8]
Working fluid	R410A	R134a
Metal foam PPI	5, 10	20, 40
Tube diameter (mm)	7.9	26
Mass flux (kg m^{-2} s^{-1})	90–270	26–106
Heat flux (kW m^{-2})	6.2–18.6	9–18
Vapor quality	0.2–0.8	0–0.9

difference is caused by the higher PPI of the metal foam in the previous study than those in the present study. In the previous study, the liquid was easily conveyed to the upper part of the tube by the high PPI metal foam to form plug flow. In the present study, the liquid does not always touch the upper part of the tube at low mass fluxes, resulting in slug flow; with the increase of mass flux and vapor quality, the liquid always touches the upper part of the tube to form plug flow.

5. Conclusions

(1) Slug flow, plug flow and annular flow were observed in metal-foam filled tubes. Slug flow and plug flow occur at vapor qualities lower than 0.4; annular flow occurs at vapor qualities higher than 0.4. With the increase of mass flux, plug flow occurs at lower vapor qualities.
(2) The metal foam promotes the formation of annular flow, and the higher PPI metal foam promotes the formation of annular flow at lower mass fluxes and lower vapor qualities.
(3) A flow pattern map was established based on the observations for the R410A two-phase flow patterns in tubes filled with 5 or 10 PPI metal foams.

Conflict of interest

None declared.

Acknowledgments

This study was supported by the National Nature Science Foundation of China (50906048), the China Postdoctoral Science Foundation (2014M560964) and the Shanghai Nature Science Foundation (15ZR1422000).

References

[1] E. Baril, A. Mostafid, L.P. Lefebvre, M. Medraj, Experimental demonstration of entrance/exit effects on the permeability measurements of porous materials, Adv. Eng. Mater. 10 (9) (2008) 889–894.
[2] A. Bhattacharya, V.V. Calmidi, R.L. Mahajan, Thermophysical properties of high porosity metal foams, Int. J. Heat Mass Transfer 45 (2002) 1017–1031.
[3] L.X. Cheng, G. Ribatski, J.R. Thome, Two-phase flow patterns and flow-pattern maps: fundamentals and applications, Appl. Mech. Rev. 61 (2008) 050802-1–050802-28.
[4] B.R. Fu, P.H. Lin, M.S. Tsou, Chin. Pan, Flow pattern maps and transition criteria for flow boiling of binary mixtures in a diverging microchannel, Int. J. Heat Mass Transfer 55 (2012) 1754–1763.
[5] B.R. Fu, M.S. Tsou, Chin. Pan, Boiling heat transfer and critical heat flux of ethanol–water mixtures flowing through a diverging microchannel with artificial cavities, Int. J. Heat Mass Transfer 55 (2012) 1807–1814.
[6] H.T. Hu, G.L. Ding, K.J. Wang, Heat transfer characteristics of R410A-oil mixture flow boiling inside a 7 mm straight microfin tube, Int. J. Refrig. 31 (6) (2008) 1081–1093.
[7] N. Kattan, J.R. Thome, D. Favrat, Flow boiling in horizontal tubes: part 1 – development of a diabatic two-phase flow pattern map, J. Heat Transfer-Trans. ASME 120 (1) (1998) 140–147.
[8] W. Lu, C.Y. Zhao, Numerical modelling of flow boiling heat transfer in horizontal metal-foam tubes, Adv. Eng. Mater. 11 (10) (2009) 832–836.
[9] J.R. Thome, Boiling of new refrigerants: a state-of-the-art review, Int. J. Refrig. 19 (7) (1996) 435–457.
[10] F. Topin, J.P. Bonnet, B. Madani, L. Tadrist, Experimental analysis of multiphase flow in metallic foam: flow laws, heat transfer and convective boiling, Adv. Eng. Mater. 8 (9) (2006) 890–899.
[11] L. Wojtan, T. Ursenbacher, J.R. Thome, Investigation of flow boiling in horizontal tubes: part I – a new diabatic two-phase flow pattern map, Int. J. Heat Mass Transfer 48 (14) (2005) 2955–2969.
[12] J.L. Xu, X.B. Ji, W. Zhang, G.H. Liu, Pool boiling heat transfer of ultra-light copper foam with open cells, Int. J. Multiphase Flow 34 (11) (2008) 1008–1022.
[13] C.Y. Zhao, Review on thermal transport in high porosity cellular metal foams with open cells, Int. J. Heat Mass Transfer 55 (13–14) (2012) 3618–3632.
[14] C.Y. Zhao, W. Lu, S.A. Tassou, Flow boiling heat transfer in horizontal metal-foam tubes, J. Heat Transfer-Trans. ASME 131 (12) (2009) 121002-1–121002-8.
[15] Y. Zhu, H.T. Hu, G.L. Ding, H. Peng, X.C. Huang, D.W. Zhuang, J. Yu, Influence of oil on nucleate pool boiling heat transfer of refrigerant on metal foam covers, Int. J Refrig. 34 (2) (2011) 509–517.
[16] Y. Zhu, H. Hu, G. Ding, S. Sun, Y. Jing, Influence of metal foam on heat transfer characteristics of refrigerant-oil mixture flow boiling inside circular tubes, Appl. Therm. Eng. 50 (1) (2013) 1246–1256.
[17] Y. Zhu, H. Hu, S. Sun, G. Ding, Heat transfer measurements and correlation of refrigerant flow boiling in tube filled with copper foam, Int. J. Refrig. 38 (2014) 215–226.